waves in BC-cut quartz show nearly identical attenuation with that of x-direction longitudinal waves. Also, Ganapolskii and Chernet's[9] measurement of the attenuation of longitudinal waves in the z direction of quartz shows the same pattern of attenuation.

In summary, we believe that the marked anomalies in the attenuation of acoustic waves peculiar to quartz are a direct result of the unusually large dispersion of the slow transverse branch.

*Work supported by the Purdue Research Foundation and the Advanced Research Projects Agency.

[1]M. Pomerantz, Phys. Rev. 139, A501 (1965).
[2]M. F. Lewis and E. Patterson, Phys. Rev. 159, 703 (1967).
[3]H. J. Maris, Phil. Mag. 9, 901 (1964).
[4]N. S. Shiren, Phys. Letters 20, 10 (1966).
[5]J. Kalejs, H. Maris, and R. Truell, Phys. Letters 23, 299 (1966).
[6]S. Simons, Proc. Phys. Soc. (London) 83, 749 (1964).
[7]M. M. Elcombe, Proc. Phys. Soc. (London) 91, 947 (1967).
[8]R. N. Thurston, H. J. McSkimin, and P. Andreatch, Jr., J. Appl. Phys. 37, 267 (1966).
[9]E. M. Ganapolskii and A. N. Chernets, Zh. Eksperim. i Teor. Fiz. 51, 383 (1967) [Soviet Phys. JETP 24, 255 (1967)].

PHYSICAL REVIEW B VOLUME 2, NUMBER 2 15 JULY 1970

Excited States in a Model Polaron Hamiltonian*

D. E. Hagen, L. L. Van Zandt, and E. W. Prohofsky
Department of Physics, Purdue University, Lafayette, Indiana 47907
(Received 14 April 1969; revised manuscript received 22 October 1969)

The energy-spectrum problem is treated for a bound stationary polaron. The Pekar Hamiltonian is used to describe the polaron and its polar lattice. This model is based on two main assumptions. First, the carrier is assumed to move much faster than the lattice ions. Second, the polaron is assumed to be spread out over a distance that is much larger than the lattice constant. These assumptions restrict us to a strong-coupling regime. A variational principle especially well suited for finding excited states has been used in a search for solutions of the polaron Hamiltonian. Using trial wave functions having s-, p-, and d-like symmetry, some well-separated approximate eigenstates of this model polaron have been found. The excited states represent internal and self-consistent excited-state solutions of the polaron Hamiltonian. It is found that the energy of each state is proportional to the square of the polaron coupling constant. Also, the qualitative features of the spectrum, i.e., the number of energy levels and their relative positions, are independent of the coupling constant.

I. INTRODUCTION

A conduction electron or a valence hole in a deformable crystal lattice creates a distortion in the over-all periodicity localized about itself. The dynamics of low-density carriers in insulators therefore involves the effects of local lattice deformations. The complex of carrier and associated deformation is a polaron. Reviews of work done on the polaron problem have been given by Appel[1] and by Kuper and Whitfield.[2] Other work relating to polaron excited states has been reported by Evrard, Devreese, and Kartheuser.[3–5]

While it is frequently convenient to consider the polaron as a single entity like a simple particle, it is clear that the many actual particles of which it is composed together with their varying interactions produce a more complex system. We expect these complexities to be made manifest in the dynamical behavior of the polaron; the polaron should show internal degrees of freedom or internal states, and these internal states should be apparent in phenomena involving energies comparable to the carrier-lattice deformation energy.

In this paper, we report the results of a theoretical search for such states. To find them more simply, we have made a number of approximations designed to reduce extraneous considerations to a minimum and focus on the carrier-lattice deformation interaction. We treat the case of the stationary polaron only, i.e., the polaron as a whole does not move through the lattice. We assume a constant optical-phonon frequency. We also assume a sym-

metric electron effective mass and dielectric constant. Effects involving transitions between polaron states giving rise to the emission and absorption of real lattice phonons are neglected.

The two main assumptions in our polaron model are the following: First, the polaron is large, i.e., spread out over a distance that is large as compared to a lattice constant. We use the effective-mass approximation to treat the basic, undistorted carrier-lattice interaction. Polaron structure with a range of the interatomic spacing is neglected. Second, we assume that the oscillation frequency of the electron in its potential well is much greater than the optical-phonon frequency of the lattice. The ions remain essentially stationary as the carrier orbits around in its potential well. These two approximations restrict us to a strong-coupling regime. A discussion of the range of coupling strengths for which these two assumptions are valid is given later.

A Hamiltonian has been written for this complex system by Pekar[6,7] on the basis of macroscopic arguments:

$$H=-\frac{\hbar^2}{2m}\nabla^2-\hbar\alpha\left(\frac{2\hbar\omega_0}{m}\right)^{1/2}\int d\vec{r}'\rho(\vec{r}')\frac{1}{|\vec{r}-\vec{r}'|}+\tfrac{1}{2}\hbar\alpha\left(\frac{2\hbar\omega_0}{m}\right)^{1/2}\int d\vec{r}\,d\vec{r}'\rho(\vec{r})\rho(\vec{r}')\left(\frac{1}{|\vec{r}-\vec{r}'|}\right), \tag{1}$$

where $\rho(\vec{r})=|\Psi(\vec{r})|^2/\langle\Psi|\Psi\rangle$ is the electron density distribution, Ψ is the electron wave function, m is the effective mass of the electron in the undistorted lattice (as opposed to its polaron mass), ω_0 is the optical-phonon frequency, α is the polaron coupling constant $\alpha=(e^2/8\pi\hbar\omega_0)(2m\omega_0/\hbar)^{1/2}(\epsilon_\infty^{-1}-\epsilon^{-1})$, ϵ_∞ is the high-frequency (optical) dielectric constant, and ϵ is the low-frequency dielectric constant.

The first term in H represents the kinetic energy of the electron. The second term represents the interaction potential between the electron and the lattice at this level of approximation. This term is negative and is the origin of the binding potential which forms the potential well in which the electron is trapped. The third term represents the polarization energy of the lattice due to the presence of the electron. It is manifestly positive.

The polaron Hamiltonian shown in Eq. (1) is nonlinear in the electron wave function. This nonlinearity is a consequence of the reduction of the polaron problem from a many-body problem involving phonons and an electron to an effective one-body problem. The reason for the nonlinearity is clear physically. The electron's wave function must appear in its own Hamiltonian because the electron is responsible for setting up the potential with which it interacts. The wave function found to satisfy Schrödinger's equation for this Hamiltonian must be the same one used to generate the potential part of the Hamiltonian.

Section II treats the energy-spectrum problem for the polaron Hamiltonian for solutions with s-wave symmetry. A variational principle especially well suited for finding excited states is used. The polaron problem is treated for solutions with p-wave symmetry in Sec. III and for solutions with d-wave symmetry in Sec. IV. The range of coupling strengths for which this theory is valid is discussed in Sec. V.

II. s-WAVE SOLUTIONS

The characteristics of a particular crystal are introduced into the polaron Hamiltonian [Eq. (1)] by the electron bare mass m, optical-phonon frequency ω_0, and the polaron coupling constant α. However, qualitative features of the energy spectrum of this Hamiltonian are independent of these terms. The relative positions and number of energy levels are also independent of the crystal under consideration. Energy levels cannot be made to appear or disappear by changing the coupling strength. This can be seen from the following scaling argument: Consider the operator $\mathcal{H}=(2m/\hbar^2)H$,

$$\mathcal{H}=-\nabla^2-\frac{\gamma}{\langle\Psi|\Psi\rangle}\int d\vec{r}'\,|\Psi(\vec{r}')|^2\frac{1}{|\vec{r}-\vec{r}'|}+\frac{\frac{1}{2}\gamma}{\langle\Psi|\Psi\rangle^2}\int d\vec{r}\,d\vec{r}'\,|\Psi(\vec{r})|^2|\Psi(\vec{r}')|^2\frac{1}{|\vec{r}-\vec{r}'|}, \tag{2}$$

where $\gamma=2\alpha(2m\omega_0/\hbar)^{1/2}$. The operators $\mathcal{H}$ and H will have the same eigenvalue spectrum except for a multiplicative factor of $(2m/\hbar^2)$. All of the information characterizing the crystal is contained in the parameter γ, which has units of (length)$^{-1}$. $\mathcal{H}$ and ∇^2 have units of (length)$^{-2}$ and $\langle\Psi|\Psi\rangle^{-1}\int d\vec{r}'\times|\Psi(\vec{r}')|^2(|\vec{r}-\vec{r}'|)^{-1}$ has units of (length)$^{-1}$. Using B to represent the integral expression, we can write the following units equation:

$$\mathcal{H}(L^{-2})=-\nabla^2(L^{-2})-\gamma B(L^{-1})\ . \tag{3}$$

If a factor k is introduced to scale the unit of length we have

$$\mathcal{H}(L^{-2})/k^2=-\nabla^2(L^{-2})/k^2-(k\gamma)B(L^{-1})/k^2\ . \tag{4}$$

The factor k can always be chosen such that $k\gamma=1$. The spectrum can be determined in this system of units and then the resulting eigenvalues can be converted to normal units in the last step. The problem is reduced to a determination of the spectrum of the operator

$$\mathcal{H} = -\nabla^2 - \frac{1}{\langle\Psi|\Psi\rangle}\int d\vec{r}'\,|\Psi(\vec{r}')|^2\,\frac{1}{|\vec{r}-\vec{r}'|} + \frac{1}{2\langle\Psi|\Psi\rangle^2}\int d\vec{r}\,d\vec{r}'\,|\Psi(\vec{r})|^2|\Psi(\vec{r}')|^2\,\frac{1}{|\vec{r}-\vec{r}'|}\ , \tag{5}$$

where $\mathcal{H}$, ∇^2, r, and Ψ are expressed in the system of units in which the unit of length is chosen so that γ is 1.

Our method is a use of a variation principle due to Frenkel.[8] The details of this principle and some other applications have been given by one of us elsewhere.[9] In this method a function θ, containing adjustable parameters, is used to approximate $\partial\Psi/\partial t$. Then the functional

$$I = \int d\vec{r}\,|H\Psi - i\hbar\theta\,|^2 \tag{6}$$

is minimized by adjusting θ. The minimization of I leads to the equation

$$\mathrm{Im}\int \delta\theta^*\,(H\Psi - i\hbar\theta)\,d\vec{r} = 0\ . \tag{7}$$

With the replacement of θ by $\dot{\Psi} = \partial\Psi/\partial t$, this becomes

$$\mathrm{Im}\int\,[\delta\dot{\Psi}^*(\vec{r},t,a_1,a_2,\ldots,a_N)/\delta a_j] \times\left(H - i\hbar\frac{\partial}{\partial t}\right)\Psi(\vec{r},t,a_1,a_2,\ldots,a_N)\,d\vec{r} = 0\ , \tag{8}$$

where the a's denote the variable parameters in the trial wave function Ψ. This is the basic equation used in the numerical calculations. One equation is generated for each adjustable parameter in the trial wave function. The resulting equations are solved simultaneously. An independent check is then performed on each solution to insure that it is indeed a minimum of the functional I shown in Eq. (6). The energy is taken from the $e^{-i\omega t}$ time dependence of the wave function or from $\langle\Psi|H|\Psi\rangle$ which is equivalent.

One of the important features of this variational principle is that it can be used directly to find excited states. It does not always find the lowest-energy state of the trial wave function as does the standard variational principle wherein $\langle\Psi|H|\Psi\rangle$ is minimized. A given trial wave function will contain adjustable parameters and will represent a certain class of functions. It can be used to find any approximate eigenfunction contained in this class of functions. Hence trial wave functions of the same general form are used in finding both the ground state and the excited states of the Hamiltonian. Each of these states will correspond to a minimum of the functional I and a corresponding best θ for the "eigenfunction."

The Frenkel variational principle was chosen for use in this problem because of its ability to find excited states directly. The ground-state solution can also be found by the Frenkel principle, however, and for this case the result is the same as that found by the standard Ritz variational principle.

The variational-principle calculations are done with the operator $\mathcal{H}$ rather than H. It is convenient to adjust the units of time so that the magnitude of $2m/\hbar$ is 1. When this is done, the variation equations take the form

$$\mathrm{Im}\int\frac{\delta\dot{\Psi}^*}{\delta a_j}\left(\mathcal{H} - i\frac{\partial}{\partial t}\right)\Psi\,d\vec{r} = 0\ . \tag{9}$$

The charge on the electron polarizes the lattice. This polarization acts back on the electron and confines the major portion of the electron density to a limited region of the crystal. Equation (1) shows that the potential energy in the effective Hamiltonian has a $1/r$ behavior far from this region. This suggests that the wave functions should have a "hydrogenlike" or decaying exponential asymptotic behavior for large $|\vec{r}\,|$. We begin, therefore, by considering s-wave states with trial wave functions of the form

$$\Psi(\vec{r},t,a_1,\ldots,a_N) = e^{-ia_N t}\,e^{-r/2a_{N-1}} \times(1 + a_1 r + a_2 r^2 + \cdots + a_{N-2}r^{N-2}). \tag{10}$$

The a's are the adjustable parameters and are assumed to be real. The parameter a_N gives the polaron energy. When this trial wave function is used in the variational principle, Eq. (9), with the operator $\mathcal{H}$ given by Eq. (5), the following set of simultaneous equations result:

$$\sum_{i,j,k=1}^{N-2} a_i a_j a_k\,\Gamma(j+k+1)\,[-(a_N' a_{N-1}^2 + \tfrac{1}{4})\,\Gamma(i+l+2) + i(l+1)\Gamma(i+l) + a_{N-1}S_{i+l+2}^{j+k}\,] = 0 \quad \text{for } 1 \le l \le N-2, \tag{11a}$$

$$\sum_{i,j,k,l=1}^{N-2} a_i a_j a_k a_l\,\Gamma(j+k+1)\,[-(a_N' a_{N-1}^2 + \tfrac{1}{4})\Gamma(i+l+2) + i(l+1)\Gamma(i+l) + a_{N-1}S_{i+l+2}^{j+k} + 2(l-1)\{-(a_N' a_{N-1}^2 + \tfrac{1}{4})\Gamma(i+l) + i(l-1)\Gamma(i+l-2) + a_{N-1}S_{i+l}^{j+k}\}] = 0\ , \tag{11b}$$

$$\sum_{i,j,k,l=1}^{N-2} a_i a_j a_k a_l\,\Gamma(j+k+1)\,[-(a_N' a_{N-1}^2 + \tfrac{1}{4})\Gamma(i+l+1) + il\Gamma(i+l-1) + a_{N-1}S_{i+l+1}^{j+k}\,] = 0\ ,$$

where $S_j^i = [(\tfrac{1}{2})^{j-1} - 1]\,\Gamma(j-1) + \sum_{l=1}^{i-1}\frac{l\Gamma(i+j-l-1)}{i\Gamma(i-l+1)}\,(\tfrac{1}{2})^{i+j-l-1}$, (12)

$$a_N' = a_N - (2\langle\Psi\,|\,\Psi\rangle^2)^{-1} \times \int d\vec{r}\,d\vec{r}\,'\,|\Psi(\vec{r})|^2|\Psi(\vec{r}\,')|^2\,\frac{1}{|\vec{r}-\vec{r}\,'|}\ , \qquad (13)$$

and Γ is the gamma function $\Gamma(j)=(j-1)!$. This set of N simultaneous nonlinear equations was truncated and solved numerically. Solutions were found corresponding to a ground state and to two excited states. All of these solutions are bound states, and they are all self-consistent under the operator $\mathcal{H}$. The ground-state solutions are given below for two-to-six-parameter wave functions:

$$\begin{aligned}
\psi_0^s &= e^{i(0.024\,41t)}\,e^{-r/6.4000}(0.001\,214\,2)\ ,\\
\psi_0^s &= e^{i(0.027\,01t)}\,e^{-r/3.7557}(0.020\,712\\
&\quad +0.009\,051\,9r)\ ,\\
\psi_0^s &= e^{i(0.027\,07t)}\,e^{-r/4.5175}(0.021\,423\\
&\quad +0.007\,365\,1r-0.000\,231\,83r^2)\ ,\\
\psi_0^s &= e^{i(0.027\,09t)}\,e^{-r/5.3660}(0.021\,726\\
&\quad +0.006\,287\,1r-0.000\,397\,63r^2\\
&\quad +0.000\,006\,033\,0r^3)\ ,\\
\psi_0^s &= e^{i(0.027\,13t)}\,e^{-r/3.4023}(0.023\,693\\
&\quad +0.006\,419\,2r+0.000\,972\,52r^2\\
&\quad -0.000\,041\,714r^3+0.000\,000\,650^3\,4r^4)\,.
\end{aligned} \qquad (14)$$

The first-excited-state solutions are given below for three-to-six-parameter wave functions:

$$\begin{aligned}
\psi_1^s &= e^{i(0.004\,097t)}\,e^{-r/20.416}\\
&\quad \times(0.008\,779\,8-0.000\,335\,43r)\ ,\\
\psi_1^s &= e^{i(0.004\,980t)}\,e^{-r/11.962}(0.003\,655\,6\\
&\quad +0.000\,871\,50r-0.000\,041\,312r^2)\ ,\\
\psi_1^s &= e^{i(0.005\,060t)}\,e^{-r/14.652}(0.003\,916\,5\\
&\quad +0.000\,685\,94r-0.000\,041\,251r^2\\
&\quad +0.000\,000\,303\,58r^3)\ ,\\
\psi_2^s &= e^{i(0.005\,120t)}\,e^{-r/11.180}(0.005\,034\,5\\
&\quad +0.000\,277\,56r+0.000\,022\,831r^2\\
&\quad -0.000\,001\,995\,1r^3+0.000\,000\,014\,908r^4)\ .
\end{aligned} \qquad (15)$$

The second-excited-state solutions are given below for five- and six-parameter wave functions:

$$\begin{aligned}
\psi_2^s &= e^{i(0.001\,948t)}\,e^{-r/22.633}(0.001\,339\,2\\
&\quad +0.000\,291\,08r-0.000\,013\,837r^2\\
&\quad +0.000\,000\,118\,83r^3)\ ,\\
\psi_2^s &= e^{i(0.002\,010t)}\,e^{-r/27.014}(0.001\,443\,0\\
&\quad +0.000\,242\,93r-0.000\,013\,058r^2\\
&\quad +0.000\,000\,151\,68r^3-0.000\,000\,000\,411\,85r^4)\ .
\end{aligned} \qquad (16)$$

In order to apply these results to real crystals, the inverse units transformations must be made. In the above work, $\gamma=2\alpha(2m\omega_0/\hbar)^{1/2}$ having units of (length)$^{-1}$ was set equal to unity. Hence, the eigenvalue a_N, of $\mathcal{H}$, having units (length)$^{-2}$, can be corrected to normal units by multiplying a_N by $\gamma^2=4\alpha^2(2m\omega_0/\hbar)$. Then this eigenvalue of $\mathcal{H}$ must be multiplied by $\hbar^2/2m$ to get the eigenvalue of H, the Hamiltonian. Hence the energy eigenvalue for a particular crystal is

$$E=(4a_N)\,\alpha^2\hbar\omega_0\ . \qquad (17)$$

For the six-parameter wave functions, we have the three self-consistent energy levels:

ground state,

$a_N=-0.027\,13$, $E_0^s=-0.1085\alpha^2\hbar\omega_0$;

first excited state,

$a_N=-0.005\,120$, $E_1^s=-0.020\,48\alpha^2\hbar\omega_0$;

second excited state,

$a_N=-0.002\,010$, $E_2^s=-0.008\,040\alpha^2\hbar\omega_0$.

The root mean square radii must be treated in a similar manner. Since the root mean square radius has units of length, it can be converted to conventional units for a particular crystal by multiplying through by $\{2\alpha(2m\omega_0/\hbar)^{1/2}\}^{-1}$. If we let $\langle r^2\rangle^{1/2}$ denote the root mean square radius in the system of units for which γ is unity, the root mean square radius for a particular crystal is given by

$$r_{\rm rms}=\langle r^2\rangle^{1/2}(\hbar/2m\omega_0)^{1/2}/2\alpha\ . \qquad (18)$$

The energy-level scheme in Fig. 1 shows the energy states for trial wave functions containing varying numbers of parameters. The three energy levels for the most accurate trial wave functions are shown again in Fig. 2. The root mean square radius has been calculated for each of the above s-state wave functions. These radii are displayed in Fig. 1. We note that the coefficient in the exponential seems to be very sensitive to the number of parameters in the trial wave function. However,

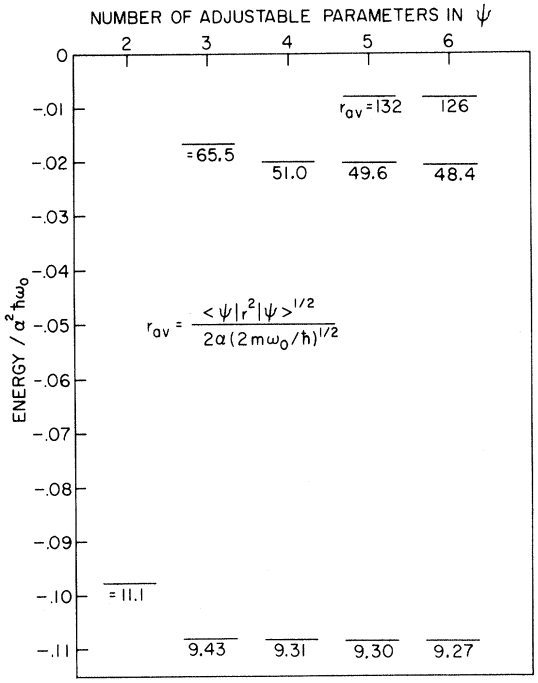

FIG. 1. Energy-level diagrams for s-wave trial wave functions containing different numbers of adjustable parameters. The root mean square radius of each level is written below that level.

quantities of interest, the energy and the polaron radius, become relatively stable and consistently decrease as the wave function of the level becomes increasingly accurate. While the exponential factor fluctuates from wave function to wave function, the product of the exponential factor and the polynomial factor is relatively stable.

The ground-state solution can be compared with the result obtained by Pekar.[6,7] Pekar used the Ritz variational principle with an exponential trial wave function and obtained the same result as our calculation. The two excited s-wave levels are new.

In the above work, it was assumed that the a's were all real. The problem was also approached under the condition that the a's appearing in the polynomial had the additional freedom to become complex. This was done because the nonlinearity of the Hamiltonian prevents one from showing that any eigenvalue could be made to correspond to a real eigenfunction. However, in this case the eigenfunctions obtained differed only by a complex over-all factor from the real wave functions. No new essentially complex solutions were found. (We have no theorem that any exist.)

III. p-WAVE SOLUTIONS

Self-consistent excited states having p-wave symmetry may also be found. This case has been treated using the Frenkel variational principle with trial wave functions of the form

$$\psi = \cos\theta\, e^{-ia_3 t}\, e^{(-r/2a_2)}\,(r + a_1 r^2/a_2)\ . \tag{19}$$

When this wave function is used in the variational principle shown in Eq. (9), the following set of simultaneous equations is generated:

$$D_{11} + a_1 D_{12} - (a_2^2 a_3' + \tfrac{1}{4})(D_{21} + a_1 D_{22}) - a_2(D_{31} + a_1 D_{32}) = 0\ , \tag{20}$$

$$(1 - 2a_1)D_{12} + a_1 D_{13} - (a_2^2 a_3' + \tfrac{1}{4})[(1 - 2a_1)D_{22} + a_1 D_{23}] - a_2[(1 - 2a_1)D_{32} + a_1 D_{33}] = 0\ , \tag{21}$$

$$D_{12} - (a_2^2 a_3' + \tfrac{1}{4})D_{22} - a_2 D_{32} = 0\ , \tag{22}$$

where

$$D_{1m} = (2 - 4a_1)\Gamma(m+3) + 3a_1\Gamma(m+4)\ ,$$

$$D_{2m} = \Gamma(m+4) + a_1\Gamma(m+5)\ ,$$

$$D_{3m} = \Gamma(m+3) + a_1\Gamma(m+4) + \{(2/5)[\Gamma(7) + 2a_1\Gamma(8) + a_1^2\Gamma(9)][\Gamma(m+1) + a_1\Gamma(m+2)] - Q_{5,m+2} - (2/5)Q_{7m} + (2/5)Q_{2,m+5} + Q_{4,m+3} + a_1[(2/5)Q_{2,m+6} + Q_{4,m+4} - Q_{5,m+3}$$

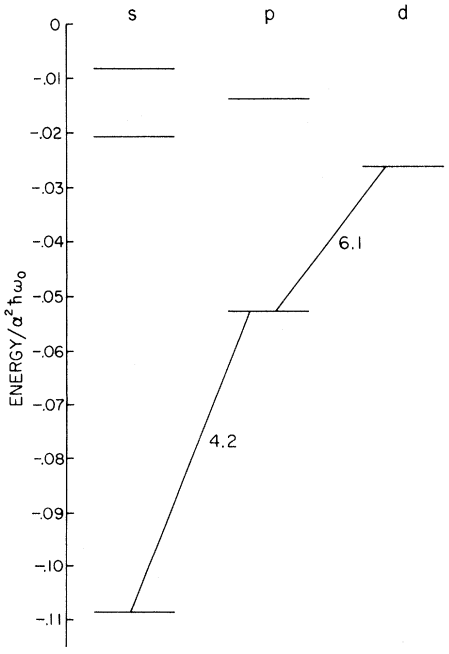

FIG. 2. Energy-level diagram showing most accurate results for trial wave functions having s-, p-, and d-like symmetries. The lower levels are connected to their nearest-neighboring levels with a line and number indicating the value of α for which the energy gap equals the phonon energy.

$$-(2/5)Q_{7,m+1}]\}/[\Gamma(5)+2a_1\Gamma(6)+a_1^2\Gamma(7)],$$

$$Q_{lm}=V_{lm}+2a_1V_{l+1,m}+a_1^2V_{l+2,m},$$

$$V_{lm}=\Gamma(l)\sum_{j=1}^{l}\Gamma(j+m)/[\Gamma(j)2^{j+m}],$$

and

$$a_3'=a_3-(2\langle\psi|\psi\rangle^2)^{-1}\times\int d\vec{r}\,d\vec{r}'\,|\psi(\vec{r})|^2|\psi(\vec{r}')|^2(1/|\vec{r}-\vec{r}'|).$$

When this set of equations is solved for the case of a two-parameter wave function, the result is $\psi_1^p=r\cos\theta\, e^{i(0.011\,75t)}\,e^{-r/9.2252}$ (0.010 068) with energy $E_1^p=-0.047\,00\alpha^2\hbar\omega_0$.

When the above simultaneous equations are solved for the case of a three-parameter wave function, the lowest p wave becomes more accurate and a second p-wave solution appears. The wave functions are

$$\psi_1^p=\cos\theta\, e^{i(0.013\,12t)}\,e^{-r/5.859\,2}(0.000\,501\,96r-0.000\,451\,48r^2), \quad (23)$$

$$\psi_2^p=\cos\theta\, e^{i(0.003\,399t)}\,e^{-r/20.897}(0.000\,576\,19r-0.000\,011\,929r^2), \quad (24)$$

and their corresponding energies are $E_1^p=-0.052\,48\alpha^2\hbar\omega_0$ and $E_2^p=-0.013\,60\alpha^2\hbar\omega_0$. The locations of these energy levels are shown on Fig. 2.

The energy of the lowest p wave has been calculated by Schultz,[10] who used the Ritz variational principle with a one-parameter Gaussian trial wave function and obtained an energy of $-0.041\times\alpha^2\hbar\omega_0$. Our calculation with the simplest wave function was 14% lower in energy. This improvement was made possible by the better asymptotic behavior of our wave function. Our most accurate result $E_1^p=-0.052\,48\alpha^2\hbar\omega_0$ is still lower because of the extra variational parameter. The second p-wave solution is new.

IV. d-WAVE SOLUTION

The polaron problem has also been treated for the case of solutions with d-wave symmetry. Here the Frenkel principle was used with a two-parameter trial wave function of the form

$$\psi=r^2P_2(\cos\theta)\,e^{-ia_2t}\,e^{-r/2a_1}, \quad (25)$$

where P_2 is the second Legendre polynomial. Only the simplest wave function was used in the d-wave investigation.

This trial wave function was used in the variational principle [Eq. (9)] to give the following set of simultaneous equations:

$$3\Gamma(6)-\Gamma(7)(a_1^2a_2'+\tfrac{1}{4})-[2a_1/\Gamma(8)][\Gamma(11)+\Gamma(9)\,\Gamma(4)+\tfrac{7}{2}\Gamma(7)\,\Gamma(6)-V_{11,1}-V_{93}-\tfrac{7}{2}V_{75}+V_{2,10}+V_{48}+(\tfrac{7}{2})V_{6,6}]=0, \quad (26)$$

$$3\Gamma(7)-\Gamma(8)(a_1^2a_2'+\tfrac{1}{4})-[2a_1/\Gamma(8)]\times[\Gamma(11)\,\Gamma(3)+\Gamma(9)\,\Gamma(5)+\tfrac{7}{2}\Gamma(7)\,\Gamma(7)-V_{11,2}-V_{94}-\tfrac{7}{2}V_{76}+V_{2,11}+V_{49}+\tfrac{7}{2}V_{67}]=0, \quad (27)$$

where

$$a_2'=a_2-(2\langle\psi|\psi\rangle^2)^{-1}\times\int d\vec{r}\,d\vec{r}'\,|\psi(\vec{r})|^2|\psi(\vec{r}')|^2(1/|\vec{r}-\vec{r}'|).$$

This set of simultaneous equations was solved to find the lowest d state. Its wave function and energy are $\psi_1^d=r^2P_2(\cos\theta)\,e^{i(0.006\,499t)}\,e^{-r/12.405}\times(0.000\,039\,562)$ and $E_1^d=-0.026\,00\alpha^2\hbar\omega_0$. The location of this level is shown in Fig. 2. The use of a trial wave function with more adjustable parameters would undoubtedly move this level down.

V. RANGE OF VALIDITY

The above polaron model is valid in the strong-coupling regime. The coupling strength is restricted in the strong-coupling limit by the assumption that the polaron is spread out over many lattice constants. As the coupling strength increases, the radius of the polaron decreases. The root mean square radius of the polaron is given above in Eq. (18). This radius must be much larger than the lattice constant a:

$$r_{\rm rms}=\langle r^2\rangle^{1/2}(\hbar/2m\omega_0)^{1/2}/2\alpha\gg a \quad (28)$$

or

$$\alpha\ll\alpha_1=\langle r^2\rangle^{1/2}(\hbar/2m\omega_0)^{1/2}/2a. \quad (29)$$

The upper limit on α is influenced by the properties of the individual crystal because of the presence of the factors a and $(\hbar/2m\omega_0)^{1/2}$.

Table I shows the restriction which the large polaron assumption places on the coupling strength. The root mean square radius is also given for each level. These results were calculated with $a=5$ Å and $(\hbar/2m\omega_0)^{1/2}=13$ Å. The s-wave results refer to the most accurate s states as determined by the six-parameter wave functions.

A lower limit is imposed on α by the basic strong-coupling assumption of a fast electron and

TABLE I. Upper limit placed on coupling strength by the large-polaron assumption. The root mean square radius is also given for each level.

State	s_0	s_1	s_2	p_1	p_2	d_1
$\langle r^2\rangle^{1/2}$	9.27	48.4	126	22.3	89.8	46.4
α_1	12	63	164	29	117	60

slow lattice particles. In order for Pekar's semiclassical polaron Hamiltonian to be valid, the frequency of the electron oscillation in its potential well must be much greater than the optical-phonon frequency. The electron oscillation frequency decreases as the coupling strength decreases.

The problem of establishing a coupling-strength criterion for the strong-coupling model has been discussed by Devreese and Evrard,[11] Hohler,[12] and by Frohlich.[13] The coupling strength must be very great, $\alpha = 9$ or 10, before the fast-electron assumption is satisfied for the ground-state polaron. It must be even higher for the excited states since they are less tightly bound in their potential wells.

Also this model neglects effects involving the emission and absorption of real lattice phonons. This requires that the gap between polaron energy levels be large as compared to the phonon energy. The energy-level separation decreases as the coupling strength decreases. When this separation nears the phonon energy, resonant transitions can occur and the energy levels will broaden and shift. In Fig. 2 the lowest levels are connected to their nearest neighbors by a line and a number indicating the value of α for which the energy separation equals the phonon energy. At $\alpha = 4.2$ the lowest s state is separated from its nearest neighbor by an optical-phonon energy. At $\alpha = 6.1$, this energy gap separates the first p level from its nearest neighbor. However, the coupling constant must already be greater than 9 or 10 for the fast-electron assumption to be valid. Hence if the coupling constant is large enough to satisfy the fast-electron assumption, it is large enough to allow real phonon emission and absorption to be neglected for the lowest levels at least.

The strong-coupling model is not well satisfied for any range of coupling strength. By the time the fast-electron assumption becomes satisfied, the large polaron assumption begins to break down. However, in the range of strong coupling, the assumptions are roughly satisfied and the polaron structure should be found.

VI. CONCLUSION

For suitable ranges of coupling strengths, this model can be used to study the internal structure of polarons. The model suggests that self-consistent excited states of polarons should exist and that indeed many states of different symmetries may exist. We have exhibited several self-consistent states within the limits of this model and have discussed the range of coupling strengths for which these states are valid. The energy of each of the states has shown the α^2 dependence characteristic of the strong-coupling case. This dependence is clearly a consequence of the assumed separation of the trial wave functions into electron and phonon parts, the assumption of the static lattice and rapid electron. The observability of these excited states depends upon their lifetimes, to which question we have not here addressed ourselves.

It was possible to compare our results with other published results at two points, the lowest s-wave state and the lowest p-wave state. Pekar[6,7] performed a variational calculation using the Ritz principle with an exponential trial wave function and obtained a result for the ground-state s-wave solution that was the same as ours. Schultz[10] performed a variational calculation using a Gaussian trial wave function with p-wave symmetry and found the energy to be $E_1^p = -0.041\alpha^2\hbar\omega_0$. Our most accurate result for the same level was 25% lower, $E_1^p = -0.0525\alpha^2\hbar\omega_0$. The improvement in our result was made possible by the use of a trial wave function with a better asymptotic behavior and with more adjustable parameters.

ACKNOWLEDGMENT

The authors wish to thank Professor G. Ascarelli for suggesting this problem and for helpful discussions.

---

*Work supported in part by the Advanced Research Projects Agency of the Department of Defense.

[1]J. Appel, in *Solid State Physics*, edited by F. Seitz and D. Turnbull (Academic, New York, 1968), Vol. 21.

[2]*Polarons and Excitons*, edited by C. Kuper and G. Whitfield (Plenum, New York, 1963).

[3]J. Devreese and R. Evrard, Phys. Letters 11, 278 (1964).

[4]R. Evrard, Phys. Letters 14, 295 (1965).

[5]E. Kartheuser, R. Evrard, and J. Devreese, Phys. Rev. Letters 22, 94 (1969).

[6]S. Pekar, Zh. Eksperim. i Teor. Fiz. 16, 341 (1946); 16, 347 (1946).

[7]S. Pekar, *Untersuchungen uber die Elektronentheorie der Kristalle* (Akademie-Verlag, Berlin, 1954).

[8]J. Frenkel, *Wave Mechanics, Advanced General Theory* (Clarendon, Oxford, 1934), p. 253.

[9]L. L. Van Zandt, Phys. Rev. 172, 372 (1968).

[10]T. D. Schultz, Technical Report No. 9, Solid State and Molecular Theory Group, MIT, Cambridge, Mass., 1956 (unpublished).

[11]J. Devreese and R. Evvard, Phys. Status Solidi 9, 403 (1965).

[12]G. Hohler, Z. Physik 140, 192 (1955).

[13]H. Frohlich, Advan. Phys. 3, 325 (1954).